in the Mo–Mo distance, 0.046 Å. This increase is entirely consistent with those previously seen in similar circumstances, namely, where one δ electron is removed from an Mo–Mo $\sigma^2\pi^4\delta^2$ configuration. In the first such case, $[Mo_2(SO_4)_4]^{4-}$ to $[Mo_2(SO_4)_4]^{3-}$, the increase was 0.056 Å,[14] and more recently for $Mo_2(tolNCHNtol)_4$ to $[Mo_2(tolNCHNtol)_4]^+$, the increase was 0.037 Å.[15]

Acknowledgment. We thank the National Science Foundation for support.

Supplementary Material Available: Fully labeled ORTEP drawings of compounds I and II, listings of the positional parameters for the hydrogen atoms in compound I, and full tables of anisotropic displacement parameters and bond angles and distances for compounds I and II (21 pages); listings of observed and calculated structure factors for I and II (44 pages). Ordering information is given on any current masthead page.

(14) Cotton, F. A.; Frenz, B. A.; Pedersen, E.; Webb, T. R. *Inorg. Chem.* **1975**, *14*, 391.

(15) Cotton, F. A.; Feng, X.; Matusz, M. *Inorg. Chem.* **1989**, *28*, 594.

Contribution from the Departments of Chemistry, SUNY Cortland, Cortland, New York, 13045, University of Virginia, Charlottesville, Virginia 22901, and James Madison University, Harrisonburg, Virginia 22807

Luminescence Studies of Pyridine α-Diimine Rhenium(I) Tricarbonyl Complexes†

LouAnn Sacksteder,‡ Arden P. Zipp,*,§ Elizabeth A. Brown,‡ Julie Streich,§ J. N. Demas,*,‡ and B. A. DeGraff*,⊥

Received January 2, 1990

The room- and low-temperature luminescences of $ReL(CO)_3X$ where L = 2,2'-bipyridine, 1,10-phenanthroline, or 5-phenyl-1,10-phenanthroline and X = substituted pyridine or quinoline were studied. Relatively small but useful variations in the state energies can be effected by altering the Hammett σ values of substituents on the pyridines. All complexes exhibit metal to ligand charge-transfer (MLCT) phosphorescences at room temperature. However, by choice of suitable ligands, the emissions can be switched to ligand-localized phosphorescence on cooling to 77 K. This behavior is explained on the basis of the proximity of the lowest MLCT and π–π^* triplet states and the changes in energy of the MLCT state as a function of temperature. At room temperature the MLCT state can equilibrate to an energy that is lower than that of $^3\pi$–π^* state and give MLCT luminescence. In rigid low-temperature media, however, the MLCT state cannot relax during the excited-state decay and emission is from the lower energy $^3\pi$–π^* state. At room temperature, lifetimes are predominantly affected by alterations in the nonradiative rate constant, as described by the energy-gap law. From σ values of the substituents, both state energies and lifetimes can be predicted before synthesis. The design of new luminescent complexes is discussed.

Introduction

Luminescent d^6 transition-metal complexes are useful as probes of macromolecular structures[1] and heterogeneous media,[2] as well as photosensitizers for solar energy conversion[3] and electron-transfer reactions.[4] While Ru(II) complexes, in particular, have been used most widely in these applications, the excited-state properties of complexes of Re(I),[5,6] Ir(III),[7] Mo(0), W(0),[8] and Os(II),[9] have been increasingly investigated. Since the metal, ligands, and solvent environment can all affect excited-state properties, variations of one or more of these factors can be used to "tune" the photophysical and photochemical properties.[10-12]

A particularly important class of luminescent complexes has been *fac*-$ReL(CO)_3X$ where L is an α-diimine ligand and X can be varied from simple ions such as Cl, Br, and CN to organic ligands such as pyridine. As part of our interest in designing specially tailored luminescent metal complexes as probes, we have examined the luminescence properties of a series of complexes where X is a substituted pyridine. We wished to determine to what extent varying the pyridine would affect the state energies, the energy degradation paths, and the radiative and nonradiative rates in the complexes.

By variation of the substituents, the basicity of the pyridines can be manipulated over 7 orders of magnitude. Given the previously demonstrated sensitivity of $ReL(CO)_3NCR^+$ to subtle structural variations in the R group,[13] we anticipated that altering the pyridines would yield large changes in the luminescence properties. We find that variations in the pyridines have a much smaller effect on the luminescence properties than we had anticipated on the basis of the wide range of electron-donor and -acceptor substituents employed. However, useful variations in properties can be effected by suitably varying the pyridine ligands.

† Presented in part at the 17th Northeast Regional Meeting of the American Chemical Society in Rochester, NY, on Nov 8-11, 1987.

‡ University of Virginia.
§ SUNY Cortland.
⊥ James Madison University.

(1) (a) Kumar, C. V; Barton, J. K.; Turro, N. J. *J. Am. Chem. Soc.* **1985**, *107*, 5518. (b) Barton, J.; Lolis, E. *J. Am. Chem. Soc.* **1985**, *107*, 708. (c) Barton, J. K.; Danishefsky, A. T.; Goldberg, J. M. *J. Am. Chem. Soc.* **1984**, *106*, 2172. (d) Barton, J. K.; Basik, L. A.; Danishefsky, A. T.; Alexandrescu, A. *Proc. Natl. Acad. Sci. U.S.A.* **1984**, *81*, 1961.

(2) Kalyanasundaram, K. *Photochemistry in Microheterogeneous Systems*; Academic Press: New York, 1987.

(3) (a) *Energy Resources through Photochemistry and Catalysis*; Grätzel, M., Ed.; Academic Press: New York, 1983. (b) Kalyanasundaram, K. *Coord. Chem. Rev.* **1982**, *46*, 159. (c) Balzani, V.; Bolletta, F.; Gandolfi, M. T.; Maestri, M. *Top. Curr. Chem.* **1978**, *75*, 1.

(4) (a) Creutz, C.; Sutin, N. *Proc. Natl. Acad. Sci. U.S.A.* **1975**, *72*, 2858. (b) Lin, C.; Sutin, N. *J. Phys. Chem.* **1976**, *80*, 97.

(5) (a) Caspar, J. V.; Sullivan, B. P.; Meyer, T. J. *Inorg. Chem.* **1984**, *23*, 2104. (b) Caspar, J. V.; Meyer, T. J. *J. Phys. Chem.* **1983**, *87*, 952.

(6) (a) Wrighton, M. S.; Morse, D. L. *J. Am. Chem. Soc.* **1974**, *96*, 998. (b) Luong, J. C.; Faltynak, H.; Wrighton, M. S. *J. Am. Chem. Soc.* **1979**, *101*, 1597. (c) Giordano, P. J.; Fredericks, S. M.; Wrighton, M. S.; Morse, D. L. *J. Am. Chem. Soc.* **1978**, *100*, 2257. (d) Fredericks, S. M.; Luong, J. C.; Wrighton, M. S. *J. Am. Chem. Soc.* **1979**, *101*, 7415. (e) Giordano, P. J.; Wrighton, M. S. *J. Am. Chem. Soc.* **1979**, *101*, 2888.

(7) (a) Watts, R. J.; Brown, M. J.; Griffith, B. G.; Harrington, J. S. *J. Am. Chem. Soc.* **1975**, *97*, 6029. (b) Watts, R. J.; Griffith, B. G.; Harrington, J. S. *J. Am. Chem. Soc.* **1976**, *98*, 674.

(8) (a) Lees, A. J. *Chem. Rev.* **1987**, *87*, 711. (b) Connor, J. A.; Overton, C.; El Murr, N. *J. Organomet. Chem.* **1984**, *277*, 277. (c) Connor, J. A.; Overton, C. *Inorg. Chim. Acta* **1982**, *65*, L1. (d) Abrahamson, H. B.; Wrighton, M. S. *Inorg. Chem.* **1978**, *17*, 3385. (e) Wrighton, M. S. *Chem. Rev.* **1972**, *74*, 401.

(9) (a) Kober, E. M.; Marshall, J. L.; Dressick, W. J., Sullivan, B. P.; Caspar, J. V.; Meyer, T. J. *Inorg. Chem.* **1985**, *24*, 2755. (b) Caspar, J. V.; Kober, E. M.; Sullivan, B. P.; Meyer, T. J. *J. Am. Chem. Soc.* **1982**, *104*, 630. (c) Kober, E. M.; Sullivan, B. P.; Dressick, W. J.; Caspar, J. V.; Meyer, T. J. *J. Am. Chem. Soc.* **1980**, *102*, 1383.

(10) (a) Watts, R. J.; Crosby, G. A. *J. Am. Chem. Soc.* **1971**, *93*, 3184. (b) Malouf, G.; Ford, P. C. *J. Am. Chem. Soc.* **1977**, *99*, 7213. (c) Ford, P. C. *Rev. Chem. Intermed.* **1979**, *2*, 267.

(11) (a) Pankuch, B. L.; Lackey, D. E.; Crosby, G. A. *J. Phys. Chem.* **1980**, *84*, 2061. (b) Pankuch, B. J.; Lackey, D. E.; Crosby, G. A. *J. Phys. Chem.* **1980**, *84*, 2068.

0020-1669/90/1329-4335$02.50/0

Table I. Absorption, Luminescence, and Electrochemical Properties of $ReL(CO)_3X^+$ Complexes

no.	complex	CT λ_{max}, nm (ϵ)	em λ_{max}, nm	τ(77 K), μs	τ_0(298 K), μs	$10^{-8}k_q$, M^{-1} s^{-1}	E_{ox}, V	$-E_{red}$, V
1	$[Re(bpy)(CO)_3(4\text{-}Me_2Npy)]^+$	388 (2100)	616	10.32	0.110	3.9	1.82[b]	1.14, 1.49
2	$[Re(bpy)(CO)_3(4\text{-}HOpy)]^+$	402 (810)	582	5.41	0.292	4.5	1.69[b]	1.21
3	$[Re(bpy)(CO)_3(4\text{-}Mepy)]^+$	364 (4000)	564	4.64	0.535	2.8	1.77	1.13, 1.39
4	$[Re(bpy)(CO)_3(3\text{-}Mepy)]^+$	364 (3500)	566	4.52	0.619	3.1	1.79	1.09, 1.39
5	$[Re(bpy)(CO)_3(4\text{-}Phpy)]^+$	364 (2800)	568	4.88	0.561	3.2	1.79	1.14, 1.49
6	$[Re(bpy)(CO)_3(py)]^+$	366 (2400)	558	4.75	0.658	2.7	1.74	1.09, 1.39
7	$[Re(bpy)(CO)_3(3\text{-}HOpy)]^+$	348 (3900)	572	4.46	0.461	3.4	1.84[b]	1.19
8	$[Re(bpy)(CO)_3(3\text{-}CH_3COpy)]^+$	346 (3300)	556	4.53	0.789	2.5	1.80	0.88,[b] 1.06,[b] 1.24, 1.50
9	$[Re(bpy)(CO)_3(4\text{-}CH_3COpy)]^+$	340 (4000)	552	4.93	0.837	2.1	1.73	0.89,[b] 1.10,[b] 1.14, 1.38
10	$[Re(bpy)(CO)_3(3\text{-}NCpy)]^+$	340 (3400)	546	4.72	0.964	2.0	1.8	1.00,[b] 1.13, 1.30
11	$[Re(bpy)(CO)_3(4\text{-}NCpy)]^+$	366 (1930)	556	4.71	0.789	2.2	1.75	1.07,[b] 1.18, 1.32
12	$[Re(bpy)(CO)_3(quin)]^+$	362 (3400)	564	1249.3	0.663	3.0	1.78	1.20, 1.43
13	$[Re(bpy)(CO)_3(2\text{-}Mepy)]^+$	364 (1600)	560	4.85	0.721	2.8	1.82	1.29, 1.55
14	$[Re(bpy)(CO)_3(3,5\text{-}Me_2py)]^+$	364 (2600)	564	4.47	0.589	3.0	1.78	1.08, 1.32, 1.48
15	$[Re(bpy)(CO)_3(2,4,6\text{-}Me_3py)]^+$	366 (2800)	566	4.83	0.585	3.2	1.84	1.20
16	$[Re(Me_2bpy)(CO)_3(py)]^+$	356 (3330)	552	4.37	0.785	4.0	1.81	1.15, 1.38
17	$[Re(Ph_2bpy)(CO)_3(py)]^+$	368 (8750)	568	4.99	1.017	2.0	1.80	0.98,[b] 1.06, 1.25, 1.36, 1.53
18	$[Re(phen)(CO)_3(py)]^+$	384 (1430)	544	9.88	1.514	2.7	1.81	1.21
19	$[Re(phen)(CO)_3(4\text{-}Mepy)]^+$	330 (4000)	552	10.01[a]	2.876	2.8	1.81	1.20
20	$[Re(5Ph\text{-}phen)(CO)_3(py)]^+$	380 (3600)	544	266.1[a]	10.569	3.6	1.83	0.98,[b] 1.14, 1.37, 1.59

[a] Multiexponential. Weighted average. [b] Irreversible.

Further tuning of properties can be obtained by altering the α-diimine.

Experimental Section

Syntheses. $ReL(CO)_3Cl$ was prepared by reacting a 10% excess of the α-diimine ligand L with $Re(CO)_5Cl$ (Pressure Chemical Co.) for 2 h in refluxing toluene under N_2. The solutions were allowed to cool before the bright yellow products were filtered, washed with toluene or hexane, and dried in air or in vacuo. These species were then converted into the pyridine derivatives by refluxing them under N_2 overnight with $AgClO_4$ and an excess of the appropriate pyridine in toluene. The AgCl was filtered out and solvent was removed in vacuo, after which the residue was dissolved in a minimum of CH_2Cl_2 and added dropwise to stirred cold pentane to precipitate the desired compounds as $[ReL(CO)_3X]ClO_4$ salts. Complexes were further purified by chromatography on Al_2O_3 using CH_2Cl_2 to elute unreacted starting material and 5% MeOH in CH_2Cl_2 to elute the product. The product was again reprecipitated by dropwise addition of a concentrated CH_2Cl_2 solution to stirred cold pentane. Table I summarizes all of the complexes studied. Microanalyses were consistent with the anhydrous complexes.

The pyridines and quinoline were from Aldrich, and the bipyridines and phenanthrolines were from Aldrich or G. Frederick Smith. The ligands and abbreviations were 4-(dimethylamino)pyridine (4-Me_2Npy), 4-hydroxypyridine (4-HOpy), 4-methylpyridine (4-Mepy), 3-methylpyridine (3-Mepy), 4-phenylpyridine (4-Phpy), pyridine (py), 3-hydroxypyridine (3-HOpy), 3-acetylpyridine (3-CH_3COpy), 4-acetylpyridine (4-CH_3COpy), 3-cyanopyridine (3-NCpy), 4-cyanopyridine (4-NCpy), quinoline (quin), 2-methylpyridine (2-Mepy), 3,5-dimethylpyridine (3,5-Me_2py), 2,4,6-trimethylpyridine (2,4,6-Me_3py), 4,4'-dimethyl-2,2'-bipyridine (Me_2bpy), 1,10-phenanthroline (phen), and 5-phenyl-1,10-phenanthroline (5-Phphen). We abbreviate complexes by listing only the diimine and the X ligand separated by a slant (e.g., 5-Phphen/py complex).

Equipment and Procedures. Absorption spectra were obtained on a Hewlett-Packard 8452 spectrophotometer. Emission and excitation spectra were recorded as described earlier.[13,14] Emission spectra were instrument- and background-corrected; excitation spectra were background-corrected. Room-temperature emission spectra were typically measured for aerated solutions (λ_{ex} = 400 nm). Low-temperature, 77 K, spectra were measured by using 1:1 MeOH–EtOH. The low-temperature phosphorescence of quinoline and 5-Phphen were measured in 4:1 MeOH–EtOH acidified with concentrated HCl by using a SPEX flash phosphoroscope.

We used the excitation spectra method described earlier[14] for assessing the presence of nonequilibrated multiple emissions. For a sample, two uncorrected excitation spectra were measured with different emission wavelengths (λ_l and λ_s). $R(\lambda)$ is calculated from

$$R(\lambda) = E_s(\lambda)/E_l(\lambda) \quad (1)$$

where the E's are the emission intensities with excitation at λ and monitoring at the long or short wavelengths (l or s). Since the sample absorbance and excitation intensities are the same at each excitation wavelength, R is related to the relative contributions of different emission components. If the sample and emission are homogeneous, E at each monitored λ arises from only one species, and $R(\lambda)$ is wavelength-independent. If there are multiple unequilibrated emissions, $R(\lambda)$ varies with λ.

This procedure can be used without low-temperature absorption spectra or calibrating the excitation output. It compensates for solvent absorption, is insensitive to solution absorbance, and works with fractured glasses. R values were only measured to 400 nm due to absorption limitations and scattering interferences with the sample emissions.

Oxygen Stern–Volmer quenching constants, K_{SV}'s, bimolecular rate constants, and emission lifetimes (τ) were measured as described elsewhere.[15-17] Decays were single exponential with no fast component at room temperature. The 77 K decays for the bpy/pyridine complexes were single exponentials with perhaps a slight suggestion of nonexponentiality for the bpy/Me_2Npy and bpy/quin complexes. However, the 5-Phphen/py and the phen/4-Mepy complexes all exhibited nonexponentiality at 77 K; emission decays were monitored near the peak of the ligand phosphorescence (≈460–494 nm) or at a wavelength that optimized the MLCT emission contribution (512–630 nm). Decays were fit to a sum of two exponentials by a nonlinear least-squares simplex program.[18]

Room-temperature luminescence quantum yields, Φ, were measured by using a Parker–Rees method with $Ru(bpy)_3^{2+}$ in deaerated water as a reference.[19] Select complexes were measured in deaerated acetonitrile. Radiative rate constants, k_r's, and lifetimes, τ_r's, were calculated from

$$k_r = \Phi/\tau \quad (2a)$$

$$\tau_r = 1/k_r \quad (2b)$$

where we have assumed that the intersystem crossing yield is unity.

Infrared spectra (KBr pellets) were obtained on a Nicolet 5DXB FTIR spectrometer.

(12) (a) Sutin, N.; Creutz, C. *Inorganic and Organometallic Chemistry*; Wrighton, M. S., Ed.; Advances in Chemistry Series 168; American Chemical Society: Washington, D.C., 1978; p 1. (b) Creutz, C.; Chou, M.; Netzel, T. L.; Okimura, M.; Sutin, N. *J. Am. Chem. Soc.* **1980**, *102*, 1309.
(13) (a) Reitz, G. A.; Dressick, W. J.; Demas, J. N.; DeGraff, B. A. *J. Am. Chem. Soc.* **1986**, *108*, 5344. (b) Reitz, G. A.; Demas, J. N.; DeGraff, B. A.; Stephens, E. M. *J. Am. Chem. Soc.* **1988**, *110*, 5051.
(14) Sacksteder, LouAnn; Demas, J. N.; DeGraff, B. A. *Inorg. Chem.* **1989**, *28*, 1787.
(15) (a) Turley, T. J. M.S. Thesis, University of Virginia, 1980; (b) Turley, T. J.; Demas, J. N.; Demas, D. J. *Anal. Chim. Acta* **1987**, *197*, 121.
(16) Buell, S. L.; Demas, J. N. *Anal. Chem.* **1982**, *54*, 1214.
(17) *Oxygen and Ozone*; Battino, R., Ed.; IUPAC Solubility Data Series, Vol. 7; Pergamon Press: Oxford, U.K., 1981.
(18) (a) Daniels, R. W. *An Introduction to Numerical Methods and Optimization Techniques*; North-Holland: New York, 1978. (b) Demas, J. N. *Excited State Lifetime Measurements*; Academic Press: New York, 1983. (c) Demas, J. N.; Demas, S. E. *Interfacing and Scientific Computing on Personal Computers*; Allyn and Bacon: New York, 1990.
(19) Van Houten, J.; Watts, R. J. *J. Am. Chem. Soc.* **1976**, *98*, 4853.

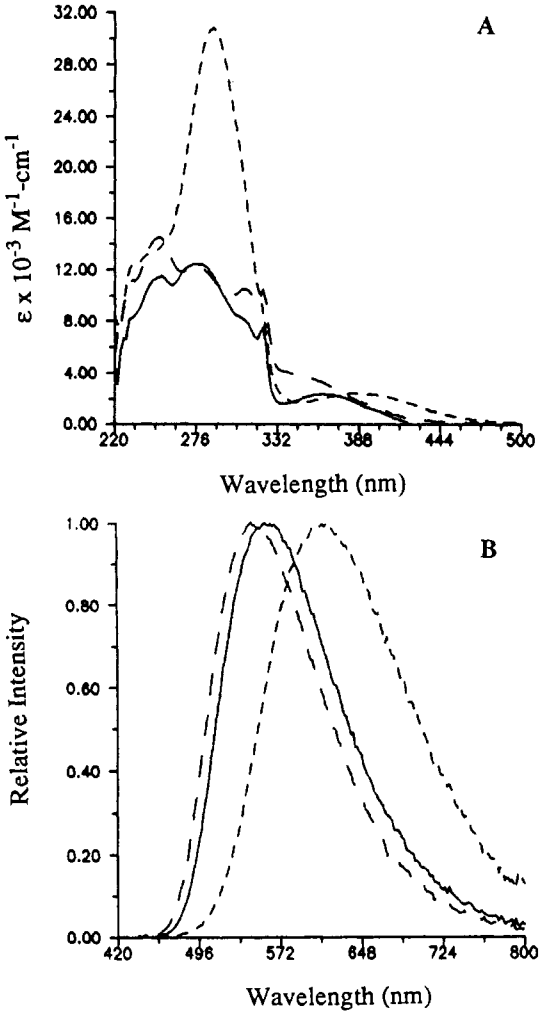

Figure 1. Room-temperature absorption (A) and emission (B) spectra of $Re(bpy)(CO)_3X$ in CH_2Cl_2: X = py (—), X = Me_2Npy (--), and X = 3-NCpy (– –).

Electrochemistry. Cyclic voltammetry measurements were made with use of a Princeton Applied Research Model 174A polarographic analyzer with a Model 200 XY recorder. All measurements were made on 2–5 mM solutions of the complexes in CH_3CN, containing 0.1 M tetraethylammonium perchlorate as the supporting electrolyte. An H-cell was used with a Pt-bead working electrode, a Pt-wire auxiliary electrode, and a saturated calomel electrode (SCE) as reference. Solutions were deoxygenated with a stream of N_2 gas and were maintained under a positive pressure of N_2 during all measurements. All potentials are reported versus the SCE.

Results

Figure 1 shows typical room-temperature absorption and emission spectra for the bpy/py, bpy/Me_2Npy, and bpy/3-NCpy complexes. The spectra are similar for all of the substituted pyridine complexes, although there are small emission shifts with the bpy/Me_2Npy complex being the most red-shifted. The room-temperature emissions are all broad and structureless.

The bpy/quinoline complex shows absorption spectra very similar to the bpy/py complexes. The quinoline $\pi-\pi^*$ singlet absorption spectrum is above 320 nm in free quinoline with an extinction coefficient of about 3000. Thus, the more intense $\pi-\pi^*$ bpy and MLCT transitions in the complex completely hide the quinoline-localized absorptions.

Figure 2 shows a plot of room-temperature emission maxima energy versus the Hammett σ value.[20] The data show an increase in emission energy with an increase in σ.

(20) (a) Murov, S. *Handbook of Photochemistry*, 2; Marcel Dekker: New York, 1973. (b) March, J. *Advanced Organic Chemistry*, 2nd ed.; McGraw-Hill: New York, 1977.

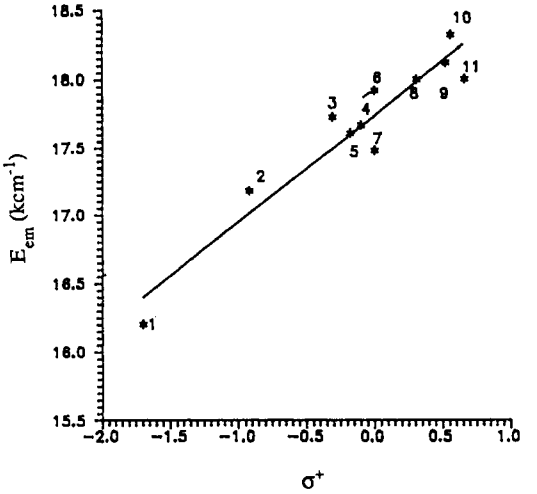

Figure 2. Plot of emission energy maxima versus Hammett σ^+ value for $Re(bpy)(CO)_3X$. The numbers correspond to the entries in Table I.

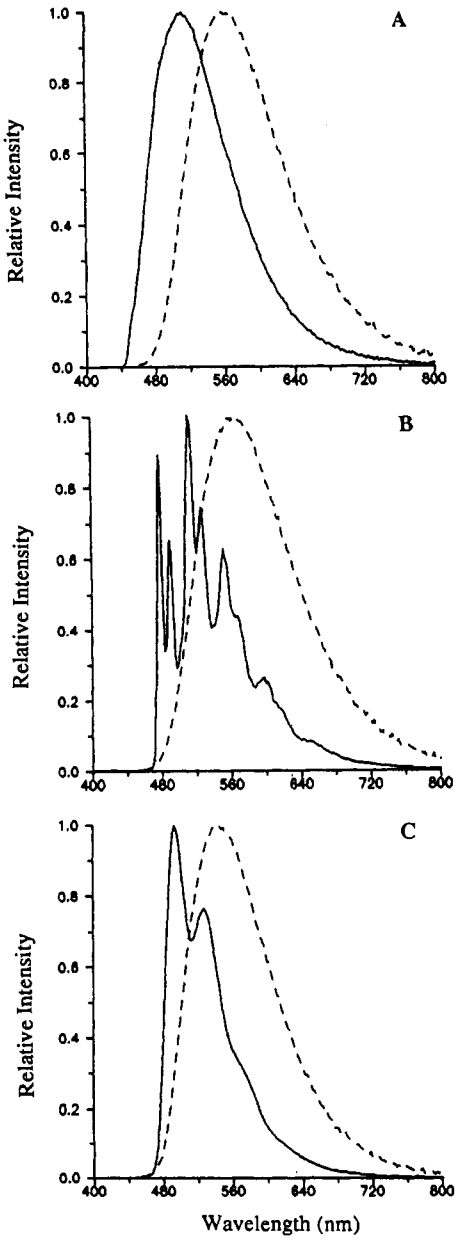

Figure 3. Room-temperature (--) and 77 K emissions (—) of (A) Re(bpy)$(CO)_3$py, (B) Re(bpy)$(CO)_3$quin, and (C) Re(5-Phphen)$(CO)_3$py.

Figure 3 contrasts the room-temperature and 77 K emission spectra for the bpy/py, bpy/quin, and 5-Phphen/py complexes. For the bpy/pyridine complexes, the low-temperature spectra are

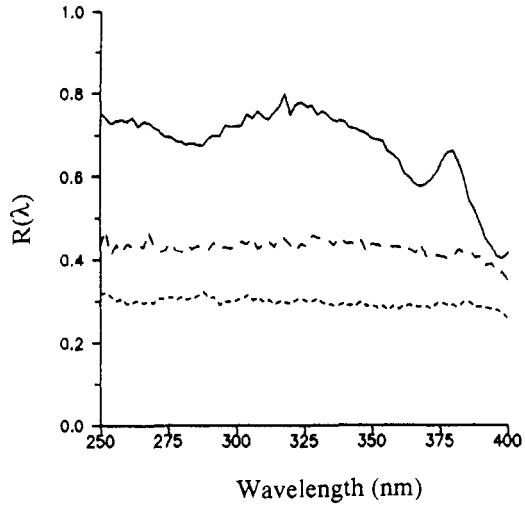

Figure 4. $R(\lambda)$ at 77 K for Re(bpy)(CO)$_3$4-NCpy (—), Re(5-Phphen)(CO)$_3$py (- -), and Re(bpy)(CO)$_3$quin (···) with monitoring at 460 and 512 nm.

broad and frequently exhibit a small shoulder on the high-energy side, at about 460 nm. While the bpy/quin and 5-Phphen/py complexes are similar to the bpy/py complex at room temperature, their emissions become highly structured at 77 K.

In general, the low-temperature emission spectra depend slightly on excitation wavelength. There were small (<5 nm) red shifts in the emission on changing the excitation wavelength from 325 to 390 nm, although the shape of the emission bands did not change appreciably. The R values determined by using the peak of the ligand and MLCT emission wavelengths were generally rather insensitive to excitation wavelength. Typical R curves are shown in Figure 4. The bpy/py complex was similar to the bpy/4-NCpy complex. Data are scaled for viewing, and the absolute R values are not significant.

For all the complexes, Table I lists the absorption and emission spectra, room- and low-temperature lifetimes, oxidation and reduction potentials, and oxygen bimolecular quenching constants. All potentials are reported versus SCE as $E_{1/2}$'s, where $E_{1/2} = 0.5(E_p^a + E_p^c)$ and E_p^a and E_p^c are the anodic and cathodic peak potentials, respectively. For irreversible waves, only the peak voltages are indicated.

All of the Re(bpy)(CO)$_3$pyX$^+$ species exhibit quasi-reversible oxidations at about 1.7–1.8 V with the exception of the bpy/3-HOpy, bpy/4-HOpy, and bpy/Me$_2$Npy complexes, which show totally irreversible behavior. Most also exhibit a series of reversible or quasi-reversible reduction waves, beginning near −1.0 V and continuing to potentials as negative as −1.6 V.

In addition to their α-diimine-based reductions, the compounds containing 3-cyano-, 4-cyano-, 3-acetyl-, and 4-acetylpyridines show at least one irreversible wave at less negative potentials, which may be associated with the cyano and acetyl groups rather than with the pyridine ring system. Compounds that contain ligands with more extended π systems (e.g., 4,4'-diphenylbipyridine and 5-phenylphenanthroline) exhibit additional reduction waves at less negative potentials.

For the nonexponential decays, there were variations in the two lifetimes and the preexponential factors. However, the two lifetimes were generally within less than a factor of 2 of each other, or one of the components contributed less than ≈10% to the total emission. These differences may arise from different sites or minor contributions from impurities. We report only the average for single-component fits to two different wavelengths.

Luminescence quantum yields were measured for representative complexes in deaerated acetonitrile. Table II shows the luminescence quantum yields, the lifetimes, and the radiative and nonradiative decay constants along with the radiative lifetimes for select complexes.

The low-temperature phosphorescence spectra of the protonated 5-Phphen and quinoline ligands were very similar to the 77 K emission spectra of the 5-Phphen/py and bpy/quin complexes, respectively, although the protonated ligands exhibited broader spectra. These results leave little doubt that the emissions of the 5-Phphen/py and bpy/quin complexes are predominantly 5-Phphen and quinoline phosphorescences, respectively.

Table II. Luminescence Properties of ReL(CO)$_3$X$^+$ in Deaerated Acetonitrile

complex[a]	Φ	τ_0, μs	$10^{-5}k_r$, s^{-1}	$10^{-6}k_{nr}$, s^{-1}	$\tau_{intrinsic}$, μs
1	0.005	0.038	1.32	26.3	7.6
6	0.059	0.241	2.45	3.91	4.1
11	0.060	0.289	2.08	3.25	4.8
12	0.046	0.263	1.75	3.63	5.7
20	0.238	2.668	0.89	0.86	11.2

[a] Numbers correspond to entries in Table I.

Discussion

Electrochemistry. The oxidation is associated with a metal-centered reaction Re(I) → Re(II). The first two reversible reduction waves are assigned to reductions of the α-diimine ligands. The potentials for these oxidations and reductions show little relationship to the basicity of the pyridines. The lack of a correlation between the oxidation potential and the donor/acceptor character of the pyridine shows that the basicity of the pyridine has minimal effect on the stability of the t_2 metal level. This absence of interaction is discussed later in the spectral sections. The lack of an effect on the reduction is not surprising given the absence of direct pyridine/α-diimine coupling.

Room-Temperature Absorption and Emission Results. The intense, high-energy absorptions (260–320 nm) for the bpy complexes are assigned to ligand π–π^* transitions analogous to those observed in protonated bpy[21] and similar Os(II) and Ru(II) bpy complexes.[22] The 340–390-nm absorption bands are assigned to a dπ(Re) → π^*(bpy) transition by analogy with a wide variety of similar α-diimine Re(I) complexes.[8a] For the phen complexes, the ligand π–π^* transitions are at ≈230, ≈260, and ≈280 nm while the ≈380-nm transition is assigned as dπ(Re) → π^*(phen). The CT character of the 340–390-nm transitions is further supported by their strong sensitivity to shifts with solvent.

The broad structureless room-temperature emissions are characteristic of MLCT emissions of Re(I) complexes, and we assign them to dπ(Re) ← π^*(bpy or phen) emissions. This is supported by the radiative lifetimes for representative complexes (Table II). These values in the low microsecond range are comparable to those observed for other MLCT emissions of similar Re(I), Os(II), and Ru(II) complexes and are much too short for a ligand-localized phosphorescence.

Low-Temperature Emission Data. The emission energies, the τ's, and the structureless 77 K emission spectra leave no doubt that all the bpy/py and phen/py complex emissions are MLCT in nature. The broad emission and the lifetimes are characteristic of MLCT emissions of Re(I) complexes.

In contrast, the bpy/quin complex exhibits a highly structured emission and has an exceptionally long lifetime (1.2 ms). The long lifetime and structure show this to be a ligand-localized phosphorescence. The emission cannot be a bpy phosphorescence because it is too far to the red (478 nm versus 448 nm for coordinated bpy in Rh(bpy)$_3^{3+}$), and the emission structure is totally different. It is, however, a good match for the phosphorescence emission energies of protonated quinoline (peaks at 478, 508, and 526 nm), although the quinoline phosphorescence is much sharper and more highly resolved in the complex than in the protonated ligand.

Similarly, the low-temperature emission of the 5-Phphen/py complex is clearly a 5-Phphen phosphorescence. This is indicated by the structure and good match to the phosphorescence of the free protonated ligand, which has peaks at 494 and 522 nm. Also, the lifetime of 0.32 ms is too long for a pure MLCT emission and must be largely a π–π^* phosphorescence.

(21) Gondo, Y.; Kanda, Y. *Bull. Chem. Soc. Jpn.* **1965**, *4*, 39.
(22) (a) Fergusson, J. E.; Harris, G. M. *J. Chem. Soc. (A)* **1966**, 1293. (b) Bryant, G. M.; Fergusson, J. E. *Aust. J. Chem.* **1971**, *24*, 275. (c) Sullivan, B. P.; Salmon, D. J.; Meyer, T. J. *Inorg. Chem.* **1978**, *17*, 3334.

The small shifts in emission energy produced by varying the excitation energy are consistent for all of the MLCT emitters. We attribute this to the complexes existing in a distribution of spectroscopically different conformations. Excitation on the red edge of the absorption photoselects conformations having lower energy MLCT absorptions and, thus, lower energy emissions. The "red-edge effect" is well-known in some organic systems.[23]

There was no red-edge variation in the low-temperature emission spectra of the bpy/quin and the 5-Phphen/py complexes. In these cases the emissions were from $\pi-\pi^*$ states whose emission energies are quite insensitive to environment. Thus, even though different molecules exist in different environments, the emissions are all virtually identical and no changes in spectra arise from photoselection of different forms.

The weak shoulder on many of the low-temperature emissions is at a wavelength consistent with a small amount of $\pi-\pi^*$ phosphorescence in the dominant MLCT emission. Thus, for the R measurements we selected wavelengths that emphasized the $\pi-\pi^*$ emission at ≈460 nm and the MLCT emission at 512 nm. The variations in R with wavelength are generally small to nonexistent (Figure 4). This indicates that even though the total emission consists of overlapping MLCT and $\pi-\pi^*$ components, there is negligible photoselection of species with different degrees of MLCT and $\pi-\pi^*$ emissions. For example, $Re(bpy)(CO)_3py$ shows no changes in R on varying the excitation from the $\pi-\pi^*$ region around 290 nm to the MLCT band at 350 nm. Thus, the emitting-state distribution is unaffected by the excitation wavelength. The exceptions to a flat $R(\lambda)$ tend to arise with very low energy excitation of species with high energy MLCT states (e.g., bpy/4-NCpy) where the MLCT state can become nearly degenerate with the $\pi-\pi^*$ level. This near degeneracy can cause slow interconversion between the two emitting states and an inhomogeneous emission.[24]

We turn now to the effect of electron-donating/electron-withdrawing power of the pyridine substituents on the spectra. Attempts were made to quantify a relationship by plotting energies versus various Hammett σ constants. The best correlations are for emission energies, especially versus σ^+ (Figure 2). Emission and absorption energies increase with an increase in the electron-withdrawing power of the pyridine substituents; more positive σ^+'s indicate more electron-withdrawing power. σ^+ is most appropriate for a situation in which a developing positive charge is important. Formation of an MLCT excited state will make the metal more positive with a resultant formation of positive charge on the pyridine ligand. Thus, ligands with more negative σ^+ values will drive electron density into the Re, make it more easily oxidized, and lower the MLCT energy.

The slope in Figure 2 is a 790 cm^{-1}/unit change in σ^+. It is surprising that this value is not larger since the basicities of these pyridines vary over 7 orders of magnitude, but the results can be accounted for in the following manner. Altering the pyridine basicity will affect the complex mainly by destabilizing the e_g d orbitals (in octahedral microsymmetry). However, the MLCT states arise from the promotion of an electron from a t_{2g} orbital, which is affected only secondarily by ligand basicity. This argument also accounts for the lack of a discernible correlation between Hammett σ values and the Re(I/II) oxidation potentials, which measures the ease of removal of an electron from a t_{2g} orbital.

The fact that emission energy shows a better correlation with σ^+ (R = 0.95) than with σ (R = 0.87) is consistent with the development of partial positive charge on the pyridine as electron density is shifted toward the Re atom. The poorer correlation with the absorption data probably arises from the difficulty of extracting accurate MLCT-state energies from broad, overlapping transitions.

There are very large variations in excited-state lifetimes with variations in the pyridine. Radiationless decay rates depend on the energies of the emitting states; the lower the energy of an emitting state, the more strongly it couples with the ground state and the larger k_{nr}. This dependence is predicted by the energy-gap law.[9b,25] Since the emission energy depends on the pyridine substituents (Figure 2), it would be reasonable to assume that our variations in τ are being controlled by the energy-gap law. To test this hypothesis, we made an energy-gap-law plot of ln k_{nr} versus E_{max}. The k_{nr} was approximated as the reciprocal of the observed lifetime, which is a good approximation for low quantum yield species. The emitting-state energy was taken as the energy of the emission maximum; while not actually equal to the state energies, it should track the state energies for a homologous series of complexes.

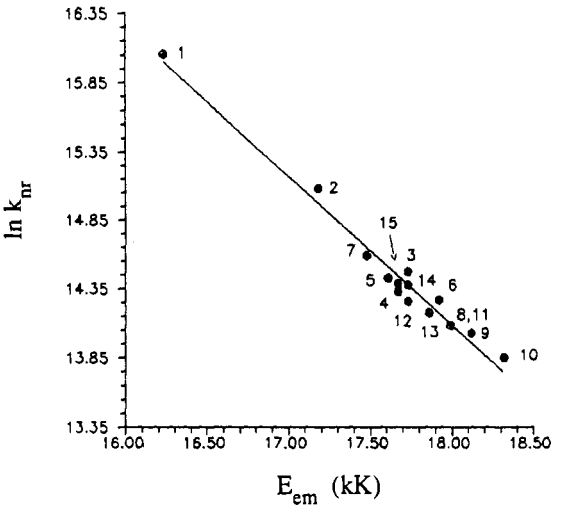

Figure 5. Energy-gap-law plot for different $ReL(CO)_3X$ species. Numbers correspond to those given in Table I.

Figure 5 shows excellent conformity to the energy-gap law and indicates that the dominant reason for the change in τ with changes in the pyridine substituents is the small decrease in emitting-state energy as electron-donating substituents are added to the pyridine. Because of the exponential relationship between the radiationless decay and energy, lifetimes are quite sensitive to the variation in σ.

We turn now to the changes in emission characteristics with temperature. All of the behavior can be accounted for in terms of the sensitivity of MLCT-state energies to solvent properties and the rates of solvent relaxation relative to the emission decay time. The MLCT-state sensitivity arises from the significant change in dipole moment that accompanies MLCT excitation. Because of this dipole moment, the MLCT excited state formed initially is nonequilibrated with respect to solvent orientation and internal geometry. It will, however, be vibrationally equilibrated for the current solvent environment, even if this is well above the thermodynamically most stable conformation. At room temperature the complex and environment can relax to the thermally equilibrated excited (thexi) state on a time scale that is short compared to the decay time. In the thexi state, the solvent and internal geometry of the complex are in their lowest energy configuration. Equilibration causes a significant drop in the energy of the initially formed MLCT state. In a rigid glass at 77 K, formation of the thexi state cannot occur during the lifetime of the excited state, and the emission will arise from the higher energy unequilibrated form. In contrast, the $\pi-\pi^*$ states in our systems do not involve large changes in dipole moment, and the ligand-state energies are largely insensitive to solvent and to relaxation processes following excitation.

We consider the different cases using Figure 6, where we show the ordering of the lowest triplet states of the systems. It is

(23) Lakowicz, J. R. *Principles of Fluorescence Spectroscopy*; Plenum Press: New York, 1983.
(24) Halper, W.; DeArmond, M. K. *J. Lumin.* **1972**, *25*, 225.
(25) (a) Kober, E. M.; Caspar, J. V.; Lumpkin, R. S.; Meyer, T. J. *J. Phys. Chem.* **1986**, *90*, 3722. (b) Caspar, J. V.; Sullivan, B. P.; Meyer, T. J. *Chem. Phys. Lett.* **1982**, *91*, 91. (c) Lumpkin, R. S.; Meyer, T. J. *J. Phys. Chem.* **1986**, *90*, 5307.

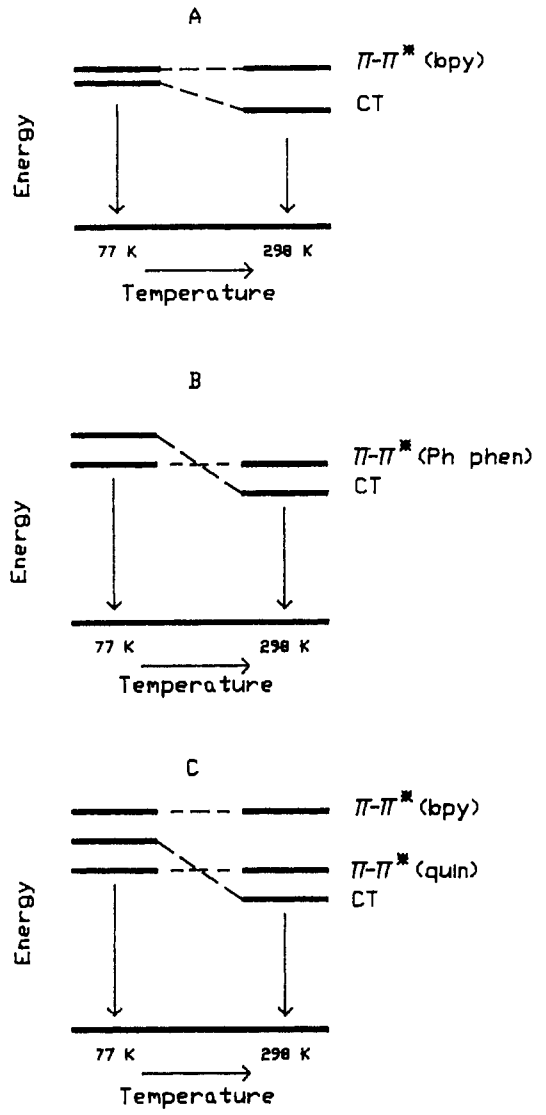

Figure 6. State diagram for lowest triplet states of (A) Re(bpy)-$(CO)_3py^+$, (B) Re(Phphen)$(CO)_3py^+$, and (C) Re(bpy)$(CO)_3quin^+$.

important to note that even at room temperature the initial MLCT-state energies are the same as the 77 K ones, but equilibration is so rapid at room temperature that the only state that can be observed in emission is the thexi state.

The majority of complexes obey case A. Their 77 K emissions are MLCT in character, which establishes that the lowest state even at 77 K is an MLCT one. At room temperature this state will drop in energy during equilibration while the $\pi-\pi^*$ state will be unchanged. Thus, at room temperature the lowest emitting state will be MLCT also, although it will be red-shifted from the 77 K emission. This is consistent with the fact that all MLCT emissions at 77 K are matched by MLCT emissions at room temperature.

The 5-Phphen/py and bpy/quin systems are strikingly different. Contrast part A of Figure 3 with parts B and C. While room temperature emissions of the 5-Phphen/py and bpy/quin complexes are MLCT, their 77 K emissions are clearly ligand-localized $\pi-\pi^*$ phosphorescences. The room-temperature MLCT emissions show that their thexi MLCT states lie below the $^3\pi-\pi^*$ state. However, the 77 K ligand phosphorescence clearly shows that the emitting ligand $^3\pi-\pi^*$ state is lower than the unrelaxed MLCT state.

The 5-Phphen/py and bpy/quin systems represent two distinct cases. The 77 K emission of the 5-Phphen/py complex is clearly the 5-Phphen phosphorescence, while the bpy/quin complex gives rise to an emission that matches that of the protonated quinoline rather than bpy. Thus, the 5-Phphen complex fits the diagram of Figure 6B while the bpy/quin case is represented by the diagram of Figure 6C. This again emphasizes that it is the lowest state in the complex, irrespective of origin, that will dominate the emission.

The low-temperature R of the bpy/quin complex is flat over the entire excitation region. Thus, even though most of the excitation at high energies (<320 nm) is going into the bpy $\pi-\pi^*$ singlet states and MLCT states and all of the excitation at longer wavelengths is going into the MLCT transitions, the emission is essentially a pure quinoline phosphorescence. Thus, interconversion between the bpy $\pi-\pi^*$ and MLCT to the emitting quinoline triplet is essentially 100% efficient. Since the lowest quinoline singlet state is at <320 nm, direct crossing from the MLCT or from the MLCT to the bpy $\pi-\pi^*$ triplet state into the quinoline triplet must be the dominant path for quinoline excitation at low excitation energies.

Conclusions

Modifying the chromophoric α-diimine ligand is a much more effective means of altering state types and energy decay paths than making changes, even major ones, in a spectator ligand such as pyridine. The spectator pyridine can only affect the state energetics by a secondary pushing or pulling of electron density into the central metal ion, which is directly involved in the excited state. However, useful state tuning can be achieved by varying the Hammett σ^+ of the pyridine substituents. The variation is estimated at a 790 cm^{-1}/unit change in σ^+. For systems with closely matched excited states of different types, such tuning could be useful for reversing the ordering of the lowest excited state and, thus, altering the emitting-state type.

Without state reordering, changes in the important luminescence quantum yields and lifetimes are predominantly affected by altering nonradiative rate constants through the energy-gap law. Thus, the price of getting a lower energy emitting state in a homologous series will be a decrease in the lifetime and quantum yield. On the basis of the σ^+ values of the substituents, both state energies and lifetimes can be predicted before synthesis. In systems with other metals and ligands, it would be necessary to build several model compounds to determine the slope and intercept of the state energy versus σ^+ plot (Figure 2) and the energy-gap-law plot (Figure 5).

Altering the spectator ligand (e.g., pyridine to quinoline) can be used to alter the energy of the lowest excited state. Extended π conjugation on the spectator ligand lowers the $\pi-\pi^*$ levels and can result in phosphorescence from the spectator ligand. Similarly, altering the π conjugation on the α-diimine ligand is useful for reordering the lowest excited states.

The variation of emitting-state type on going from room temperature to 77 K is accounted for completely by the freezing (77 K) of the facile relaxation of MLCT states to their lower energy thexi states. At room temperature the thexi state is readily formed with a large drop in MLCT energy, while at 77 K the MLCT state cannot relax on the time scale of the emission; thus, state reordering relative to room temperature can result. This feature can be used to tune emitting levels.

Acknowledgment. We gratefully acknowledge support by the National Science Foundation (Grants CHE 86-00012 and 88-17809). We thank Hewlett-Packard for the gift of the 8452 spectrometer, Mr. Henry Wilson for his assistance, and students in our Physical Chemistry Laboratory for preliminary measurements.